

Influence of Carbon Vacancies on CO Chemisorption on TiC(001): A Theoretical Study

Dae-Bok Kang

Department of Chemistry, Kyungsung University, Busan 48434, Korea

E-mail: dbkang@ks.ac.kr

(Received October 10, 2016; Accepted November 7, 2016)

ABSTRACT. The extended Hückel method is employed to analyze the interaction of carbon monoxide with the TiC(001) surfaces, both perfect and containing carbon vacancies. CO exhibits a similar σ -donation interaction for both $\text{Ti}_{25}\text{C}_{25}$ and $\text{Ti}_{25}\text{C}_{23}$ clusters, as deduced from the fact that the populations of the CO 5σ orbital are identical upon adsorption, but it bonds more strongly with the $\text{Ti}_{25}\text{C}_{23}$ than with the $\text{Ti}_{25}\text{C}_{25}$ because the metal d electron density in $\text{Ti}_{25}\text{C}_{23}$ provides π back-bonding interactions with CO that are absent in $\text{Ti}_{25}\text{C}_{25}$. This work suggests that a difference in reactivity toward CO of stoichiometric TiC and TiC with carbon defects is connected with the occupancy of $2\pi^*$ orbitals that leads to a significant weakening of the C-O bond.

Key words: Titanium carbide, Adsorption, Electronic structure, CO

INTRODUCTION

Surface chemical reactivity of the transition metal carbides has attracted interest for their catalytic properties similar to many metal surfaces.^{1,2} These properties result from the electronic structure of these materials. In this paper, we focus on the electronic structure and surface chemical interaction of titanium carbides that are critical in their successful use as catalysts. These substrates exhibit a difference in reactivity toward CO, which has been used as a probe molecule of chemical activity for both metal and metal carbide catalysts. In order to analyze the bonding and surface reactivity with CO, we present the results of extended Hückel (EH) cluster and band structure calculations for the electronic properties of TiC(001) surfaces, both perfect and containing carbon vacancies. Contrary to the case of metal surfaces, limited theoretical studies of CO adsorption have been performed on TiC(001) surface. Didziulis et al. used density functional theory (DFT) to examine interactions of CO with TiC(001).^{3,4} They report that CO adsorption on TiC(001) prefers on top Ti sites. Depending on the cluster model selected, the adsorption energies of CO are quite different. Work performed on small clusters predicted weak adsorption energy of 0.55 eV, which is interpreted as arising from the σ -donation bonding of the CO 5σ orbital with the empty metal d_{z^2} orbital.

The strength of the surface bond with CO and the tendency for CO to dissociate are strongly associated with the extent of metal-to-CO π back-bonding interactions. Our calculations show that CO molecules form a fairly strong Ti-C π back-

bonding with the surface when adsorbed on atop Ti sites of the TiC(001) containing C vacancies. We investigate in this paper how the bonding situation is influenced by the vacancies on the carbon sublattice. The effect of C vacancies on the chemical reactivity of the TiC(001) surface is discussed in terms of the density of states (DOS) and the fragment molecular orbital (FMO) populations. We also report quantitatively the strength of metal-CO and C-O bonds by use of the integrated overlap populations up to the Fermi level. All the calculations in this work have been performed with the CAESAR program package;⁵⁻⁷ atomic parameters are given in *Table 1*.

RESULTS AND DISCUSSION

A two layer thick $\text{Ti}_{25}\text{C}_{25}$ slab is used to represent the TiC(001) surface with a stoichiometric composition, as depicted in *Fig. 1*. The $\text{Ti}_{25}\text{C}_{23}$ slab with carbon vacancies is modeled by removing two carbon atoms denoted by V in the first layer of the TiC(001) surface. The experimental lattice parameter ($a = 4.32 \text{ \AA}$) for the cubic rocksalt-type TiC is employed in the calculations. The Ti-C nearest neighbor distance is 2.16 \AA . No surface reconstructions are considered. The C-O bond length of 1.14 \AA is kept constant for all calculations. For the surface-CO interactions, the Ti-CO bond distance is 2.20 \AA in both clusters.^{3,4} Usually the metal-CO bond is described in terms of the Blyholder model,⁸ which involves electron donation from the CO 5σ orbital to the metal and the back-donation from the metal to the CO $2\pi^*$ orbitals. In the CO bonded clusters, carbon monoxide can interact

Table 1. Parameters for EH calculations

atom	orbital	H_{ii} , eV	ζ_1^b	ζ_2^b	c_1^a	c_2^a
Ti	3d	-7.18	4.55	1.40	0.4206	0.7839
	4s	-6.52	1.50			
	4p	-3.81	1.50			
C	2s	-21.4	1.625			
	2p	-11.4	1.625			
O	2s	-32.3	2.275			
	2p	-14.8	2.275			

^aCoefficients used in double- ζ expansion. ^bSlater-type orbital exponents.

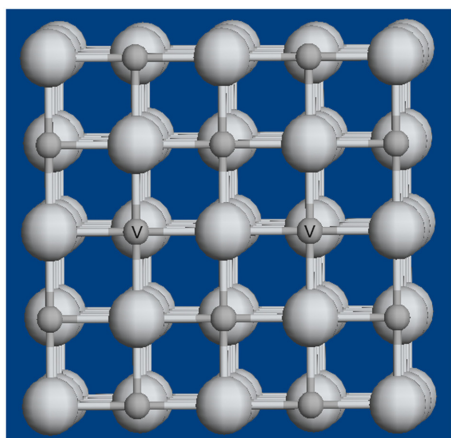


Figure 1. Top view of the 2×2 supercell model for the TiC(001) surface of the rock-salt structure. Big and small spheres represent Ti and C atoms, respectively. In the case of TiC(001) with carbon defects, the two carbon atoms are replaced with vacancies denoted by V.

with the substrates as the σ -donor and π -acceptor molecule, exhibiting a similar interaction as is expected for metal surfaces. We use the model to examine the interaction of a CO molecule with the metal site of both clusters.

Molecular orbital calculations were performed on the free CO molecule, the TiC(001) cluster, and the cluster-CO system. Adsorption energies (E_{ad}) are obtained by subtracting the energy of the combined cluster-CO system from the sum of the energies of the free CO molecule and the cluster. The EH calculations produce adsorption energies that are unrealistic and provide only qualitative predictions for the adsorption energy. The results of calculations on the bonding of CO with these clusters are summarized in *Table 2*.

Table 2. Results from the TiC-CO cluster calculations

cluster	Ti-CO bond (\AA)	C-CO bond (\AA) ^a	E_{ad} (eV)
Ti ₂₅ C ₂₅	-	1.32	-1.72
Ti ₂₅ C ₂₅	2.20	-	1.63
Ti ₂₅ C ₂₃	2.20	-	7.37

^aTaken from refs. 9, 10.

On the Ti₂₅C₂₅ cluster, the adsorption energy of CO on Ti and C sites is estimated to be 1.63 eV and -1.72 eV, respectively. As might be expected, bonding of CO with carbon end down is more stable on a titanium site than a carbon site of the cluster. For an on top adsorption of CO on Ti, we calculate much stronger adsorption energy for Ti₂₅C₂₃ relative to the Ti₂₅C₂₅ cluster. The primary reason for this is due to the π back-bonding of the defective cluster with the CO molecule. Thus the strength of CO bonding to surfaces depends on the back-donation of electrons from surface into the CO $2\pi^*$. Assuming the z -axis perpendicular to the surface, the occupied Ti $3d_{xz,yz}$ orbitals in Ti₂₅C₂₃ participate in the π back-bonding interaction with the empty $2\pi^*$. This interaction is not possible in Ti₂₅C₂₅, because this cluster has no occupied Ti 3d orbitals. The occupation of CO $2\pi^*$ orbitals is confirmed in *Table 3*. The strengths of the CO σ -donation bond to the unoccupied dz^2 level are comparable on both clusters, as deduced from the fact that the populations of the CO 5σ orbital are identical upon adsorption.

Table 3 also contains the calculated Mulliken charges on the CO molecule involved in the cluster-CO bond. The charge plays an important role in the relative donor and acceptor interactions of the cluster. The positive charge on the CO molecule for the Ti₂₅C₂₅ cluster has been increased slightly from a zero charge value of the free molecule, consistent with the σ -donation bonding of CO. Adsorption of

Table 3. Relevant overlap populations, FMO occupations, and charges for CO on TiC(001)

	TiC	TiC _{0.94}
FMO occupations		
5σ	1.77	1.77
$2\pi^*/\text{orbital}$	0.08	1.64
CO charge	+0.18	-2.94
Overlap populations		
C-O	1.32	0.43
Ti-CO	0.52	0.83

CO on the stoichiometric TiC ($\text{Ti}_{25}\text{C}_{25}$ cluster) occurs only through its σ -donation to Ti d^0 sites. On the other hand, CO gains some electrons from the $\text{Ti}_{25}\text{C}_{23}$ cluster and is reduced significantly. The large negative charge of CO indicates its back-bonding interaction with the Ti atom of the cluster with carbon defects. The presence of electron density in the metal d orbitals of $\text{Ti}_{25}\text{C}_{23}$ is critical in understanding the difference in reactivity for CO between the two clusters. In the stoichiometric solid, the formally assigned charges are $\text{Ti}^{4+}\text{C}^{4-}$. The requirement of charge neutrality results in the decrease in the oxidation state of Ti from +4 to +3.68 as C vacancies increase from the $\text{Ti}_{25}\text{C}_{25}$ to $\text{Ti}_{25}\text{C}_{23}$. The introduction of carbon vacancies in the TiC(001) structure facilitates the formation of reduced Ti^{3+} cations and hence leads to the population of the metal d orbitals on the surface. Consequently, $\text{Ti}_{25}\text{C}_{23}$ has more electrons at Ti 3d orbitals than $\text{Ti}_{25}\text{C}_{25}$. This occupation of Ti 3d orbitals strengthens the π back-bonding interaction between CO and Ti of the $\text{Ti}_{25}\text{C}_{23}$ cluster.

Band structure calculations were performed to move beyond the limitations of the cluster calculations. In general, this approach for crystalline materials generates many of electronic features that are consistent with the cluster models. A two-dimensional (2D) slab that is four layers deep is repeated in a supercell geometry. This supercell is derived from the cubic unit cell containing four formula units. The 2×2 supercell model has eight Ti and eight C atoms in each layer (64 atoms in total) for stoichiometric TiC, as shown in Fig. 1. To address the influence of C vacancies on the chemical reactivity of the surface, the TiC with carbon defects is also considered. The defective 62 atom supercell with two C atoms replaced by vacancies can be represented as nonstoichiometric $\text{TiC}_{0.94}$. Only these repeating units are considered in the calculations.

Fig. 2a shows the total DOS and the carbon and titanium contributions to the DOS calculated for TiC. The general characteristics of the bands, in order of increasing energy, is C 2s (-21.5 to -23 eV), C 2p (-11 to -13.5 eV), and Ti 3d. The covalent nature of the bonding is manifested by the significant admixture of the Ti 3d levels with C 2p orbitals. The Ti 3d levels have a small amount of electron density in the C 2p band below the Fermi level and thus are little populated. The C 2p levels are completely filled.

We present the DOS for an ordered model structure of the carbon deficient $\text{TiC}_{0.94}$ in Fig. 2b and discuss the interesting changes which occur in comparison with stoichiometric TiC. The $\text{TiC}_{0.94}$ populates low lying Ti 3d levels that are formally unoccupied in TiC. The total DOS curves are similar, but the Fermi levels are quite different for the

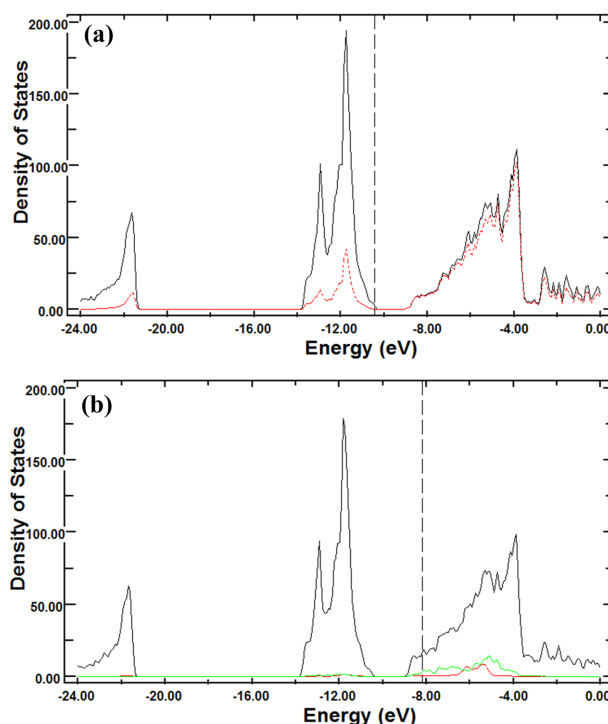


Figure 2. (a) Contributions of (a) Ti 3d (red line), (b) surface Ti d_{z^2} (red line) and $d_{xz,yz}$ (green line) orbitals to the total DOS of (a) TiC(001) and (b) $\text{TiC}_{0.94}$ (001). The dashed vertical line indicates the Fermi level.

two carbides. There is a shift of the Fermi level to higher energy in $\text{TiC}_{0.94}$ compared with TiC. In stoichiometric TiC, the formal charge of C is -4 . The surface carbon atoms are electron-rich, since C is more electronegative than Ti. But carbon is neutral as it is removed. As with C vacancies on the surface, some metal states in the Ti 3d band become occupied and become available for surface-CO bonding. The DOS from the $\text{TiC}_{0.94}$ shows the occupied metal $d_{xz,yz}$ states to participate in bonding interactions with CO $2\pi^*$. This presents a significantly different environment for CO to gain electron density from the surface.

A single CO molecule is assumed to occupy an on top Ti site at the center of the supercell model, resulting in a $1/8$ coverage with respect to surface Ti atoms. This provides an overall coverage of $1/16$ for the perfect surface and an adsorbate-adsorbate separation of 8.64 \AA . The repulsive lateral interaction between neighboring CO molecules is not included in this calculation. The 5σ orbital of CO has been stabilized by about 0.9 eV by bonding to the surface of either carbide. This is due to the σ -overlap between the CO 5σ orbital and the empty Ti $3d_{z^2}$ orbital with which it interacts. As the $3d_{z^2}$ levels are unoccupied, only the bonding levels are occupied in the interaction of CO with these surfaces. Since the 5σ of CO is a carbon lone-pair

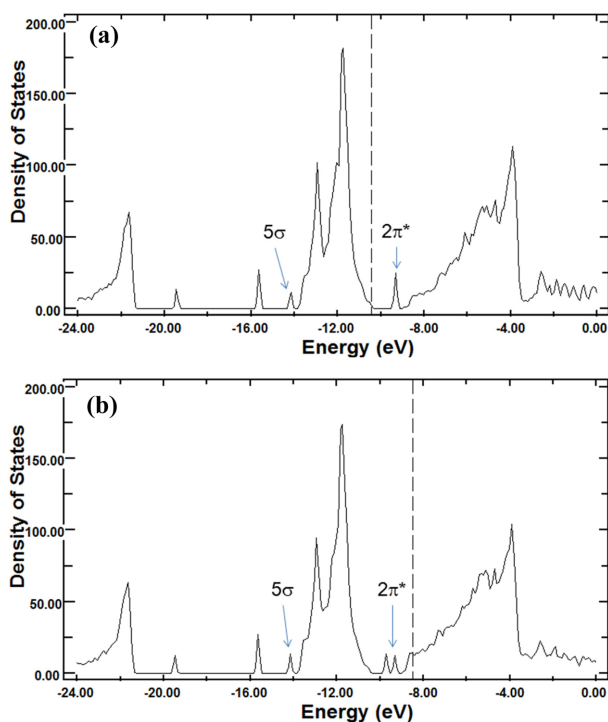


Figure 3. DOS with 5σ and $2\pi^*$ projections for CO on (a) TiC(001) and (b) TiC_{0.94}(001). The dashed vertical line indicates the Fermi level.

orbital, it can participate effectively in σ -donor bonding to the surface. The other major bonding interaction for CO adsorption is the π back-donation from the metal $d_{xz,yz}$ orbitals to the CO $2\pi^*$. These interactions can be observed in the DOS plots for the metal orbitals and relevant CO orbitals in Fig. 3. The $d_{xz,yz}$ - $2\pi^*$ bonding levels in TiC_{0.94} are occupied to a greater extent and contribute significantly to the surface bond of CO, whereas these levels in TiC are just above the Fermi level and do not contribute to the CO bonding. The energy stabilization of the $2\pi^*$ orbitals is indicative of a stronger surface-CO bond for the CO bound TiC_{0.94}. The greater dispersion is also observed for the $2\pi^*$ band of CO on TiC_{0.94}. This dispersion reflects a more covalent bonding interaction between the surface Ti $3d_{xz,yz}$ and the $2\pi^*$.

The back-bonding from Ti $3d_{xz,yz}$ into the CO $2\pi^*$ contributes to weakening of the C-O bond, strengthening the Ti-CO bond. This interaction can be followed by large Ti-CO overlap populations and significant populations of the CO $2\pi^*$ which may be an initial indicator of CO dissociation. The carbon deficient surface displays an enhanced reactivity toward CO, which is manifested in stronger Ti-CO and weaker C-O bonding. The relevant overlap populations and electron densities are presented in Table 3. A significant reduction is seen in the C-O overlap population rel-

ative to that of the free molecule. The overlap population falls from 1.35 in free CO to 0.43 at this surface. However, no such π back-bonding of CO is expected for the TiC because the $d_{xz,yz}$ - $2\pi^*$ bonding levels are unoccupied. Thus, the $2\pi^*$ orbitals of CO are little populated. The small occupation of the $2\pi^*$ occurs through the Ti mixing into the carbon 2p band. There is no significant reduction in the overlap population of the C-O bond on TiC. The s -donation from the CO $5s$ orbital into surface Ti dz^2 orbital does not affect the bond strength of the molecule. Therefore, the (001) surface of stoichiometric TiC does not weaken the C-O bond significantly. Although no experimental studies have been reported for the bonding of CO to the surface with C defects, the carbon deficient surface whose metal d orbitals are partially occupied is expected to be more active for CO adsorption than is the perfect surface. The effect of creating carbon vacancies on TiC(001) surface would be a very promising way to enhance the activity toward CO of the surface.

CONCLUSION

A simple molecular orbital framework was used to understand the chemical activity toward CO of the (001) surface of TiC. This analysis provides the details of interactions of CO with the surface which demonstrate differences in reactivity due to surface composition. The effect of removing carbon atoms to activate the surface is explored in this study. The metal site of stoichiometric TiC is only capable of weak σ -donation bonding by CO due to a lack of available d electrons for π back-bonding interactions. The presence of metal d electron density in the TiC(001) with C defects adds greater stability to the surface-CO bond by a back-bonding interaction with CO $2\pi^*$ and hence increases an occupancy of the $2\pi^*$ orbitals. This results in a significant weakening of the C-O bond and enhanced catalytic activity toward CO of the titanium carbide.

Acknowledgment. Publication cost of this paper was supported by the Korean Chemical Society.

REFERENCES

- (a) Levy, R. L.; Boudart, M. J. *Science* **1973**, *181*, 547.
(b) Hwu, H. H.; Chen, J. G. *Chem. Rev.* **2005**, *105*, 185.
- Oyama, S. T. *The Chemistry of Transition Metal Carbides and Nitrides*; Blackie Academic and Professional: Glasgow, U.K., 1996.
- Didziulis, S. V.; Butcher, K. D.; Perry, S. S. *Inorg. Chem.* **2003**, *42*, 7766.

4. Didziulis, S. V.; Frantz, P.; Fernandez-Torres, L. C.; Guenard, R. L.; El-bjeirami, O.; Perry, S. S. *J. Phys. Chem. B* **2001**, *105*, 5196.
 5. Whangbo, M.-H.; Hoffmann, R. *J. Am. Chem. Soc.* **1978**, *100*, 6093.
 6. Whangbo, M.-H.; Hoffmann, R.; Woodward, R. B. *Proc. R. Soc. A* **1979**, *366*, 23.
 7. Ren, J.; Liang, W.; Whangbo, M.-H. *Crystal and Electronic Structure Analysis Using CAESAR*; 1998. For details, see: <http://www.PrimeC.com/>.
 8. (a) Blyholder, G. *J. Phys. Chem.* **1964**, *68*, 2772. (b) Sailer, J.-Y.; Hoffmann, R. *J. Am. Chem. Soc.* **1984**, *106*, 2006.
 9. Mant, B. P.; Asara, G. G.; Anderson, J. A.; Homs, N.; Ramirez de la Piscina, P.; Rodriguez, S.; Ricart, J. M.; Illas, F. *Surf. Sci.* **2013**, *613*, 63.
 10. Asara, G. G.; Feria, L.; Florez, E.; Ricart, J. M.; Liu, P.; Rodriguez, J. A.; Illas, F. *J. Phys. Chem. C* **2011**, *115*, 22495.
-